Structural Engineering and Mechanics, Vol. 6, No. 3 (1998) 347-362
DOI: http://dx.doi.org/10.12989/sem.1998.6.3.347

Seismic and vibration mitigation for the A-type offshore template platform system

Hsien Hua Lee†

Department of Marine Environment, National Sun Yat-sen University, Kaohsiung, Taiwan, R.O.C.

Abstract. In this study an improved design method for the traditional A-type (or V-type) offshore template platform system was proposed to mitigate the vibration induced by the marine environmental loadings and the strong ground motions of earthquakes. A newly developed material model was combined into the structural system and then a nonlinear dynamic analysis in the time domain was carried out. The analysis was focused on the displacement and rotation induced by the input wave forces and ground motions, and the mitigation effect for these responses was evaluated when the viscoelastic damping devices were applied. The wave forces exerted on the offshore structures are based on Stokes fifth-order wave theory and Morison equation for small body. A step by step integration method was modified and used in the nonlinear analysis. It was found that the new design approach enhanced with viscoelastic dampers was efficient on the vibration mitigation for the structural system subjected to both the wave motion and the strong ground motion.

Key words: offshore structure; dynamic analysis; viscoelastic material; vibration mitigation; seismic mitigation.

1. Introduction

Vibration induced by the lateral loadings such as the wind loadings, or strong ground motions due to earthquakes usually causes excessive deflection and damage to the structures. Offshore structures are the typical ones subjected to tremendous lateral loadings such as the overwater wind, surface waves, currents during severe storm conditions, and strong ground motions from earthquakes. The damages caused from these dynamic loadings are usually substantial. In order to mitigate the vibration and then avoid serious damage, a new mechanical damping device, which has substantial energy absorption ability, was incorporated in the structural system. Experimental testing for both of the material properties and the structural systems incorporated with damping devices have been carried out and shown that viscoelastic dampers have significantly improved the dynamic performance of the structures (Mahmoodi 1972, Bergman and Hanson 1986, Lin, *et al.* 1988, Chang, *et al.* 1991). According to the test data, substantial energy input into the structural system can be absorbed by this damping material. Although the encouraging mechanical properties of the material were observed in the laboratory, it is usually difficult to have an adequate evaluation and design for the structural system when the mechanical behavior of the damping devices can not be predicted appropriately. To solve this problem, an analytical material model for this viscoelastic damper, which can accurately describe the mechanical behavior, was developed by Lee and Tsai (1992, 1994). With this model, evaluations for

† Associate Professor

some typical structural systems associated with the damping devices were carried out (Tsai and Lee 1992a, b, 1993a, b), and good results for dynamic performances were obtained.

Template structure is a common type of infra-structure being widely used for engineering structures in the marine environment, such as the petroleum production complex, radar station, and some other facilities for navigation purposes. A study on the dynamic behavior of the template structure incorporated with the viscoelastic damping device was also performed lately (Lee and Wu 1996). It showed that some degrees of upgrading in the dynamic characteristics was obtained when the offshore platform was subjected to the wave motions. In that analysis, the proposed viscoelastic devices were installed in the diagonal bracings, as were used in the high-rise buildings. However, this design for the structure in the marine environment might suffer from stability problem, particularly when the template structure is subjected to the out-of-plane transverse wave forces. Therefore, in this study, a typical A-type (or V-type) template platform was selected and redesigned with improved method for the mechanical dampers that were installed at the joint between the horizontal and inclined bracing members. This new design could well avoid the buckling of the bracing members as might occur in the previous design, where the damping devices were installed in between two separated parts of the diagonal bracings.

In this study the strong ground motion was also taken into account and combined in the equation of motion for the offshore structural system since the on-field investigation (Mason, *et al.* 1989) showed that substantial deflections were observed for the offshore structures under earthquakes. The nonlinear analysis in the time domain was then carried out for this offshore structural system subjected to the marine environmental loadings and strong ground motions. The purposes of this study are to develop an alternative method that could well avoid the bracing buckling for the application of the viscoelastic dampers to the offshore template structures, and further to find the vibration mitigation effect for both the wave motions and the random type ground motions when the newly developed material model was incorporated in the analysis.

2. Finite element formulation for viscoelastic damper

In order to adequately predict the behavior of structural material subjected to dynamic loading, an analytical model must be capable of representing the typical material characteristics and adequately describing the dynamic behavior. Based on the molecular theory and the fractional derivative viscoelastic model (Bagley and Torvic 1979), a nonlinear analytical model was derived and modified by using the available experimental results (Lee and Tsai 1992, 1994). For the linear variation of the strain between two time steps, $(n-1)\Delta t$ and $n\Delta t$, the constitutive law for the viscoelastic damper at time step $n\Delta t$ is presented as

$$\tau(n\Delta t)=\left[G_0+\frac{G_1(\Delta t)^{-\alpha}}{(1-\alpha)\Gamma(1-\alpha)}\right]\gamma(n\Delta t)+\tau_p(n\Delta t) \qquad 0<\alpha<1, \tag{1}$$

where τ and γ are the stress and strain of the material; G_0 and G_1 represent the shear modulus corresponding to the storage and the loss energy, respectively, and $\Gamma(1-\alpha)$ is the gamma function while α is a fractional number corresponding to the material properties. The previous time effect of the strain, $\tau_p(n\Delta t)$, is defined as

$$\tau_p(n\Delta t)=\frac{G_1\Delta t^{-\alpha}}{(1-\alpha)\Gamma(1-\alpha)}\left(W_0^n\gamma(0)+\sum_{i=1}^{n-1}W_i^n\gamma(i\Delta t)\right) \tag{2}$$

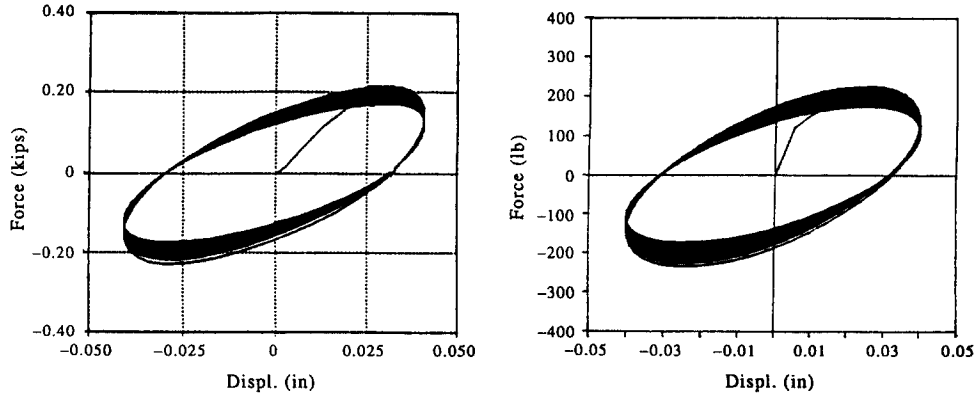

(a) Experimental data (b) Analytical results

Fig. 1 Typical force-displacement relationship for the damping material (after Lee and Tsai 1994).

where W_0^n and W_i^n are weighting functions corresponding to the time steps as

$$W_0^n = (n-1)^{1-\alpha} + (-n+1-\alpha)n^{-\alpha}, \quad 0 < \alpha < 1 \tag{3}$$

and

$$W_i^n = -2(n-i)^{1-\alpha} + (n-i+1)^{1-\alpha} + (n-i-1)^{1-\alpha}. \tag{4}$$

The degradation of the shear modulus and the thermal effect are taken into consideration in this material model. A typical force-displacement relationship representing the mechanical behavior of the viscoelastic material is shown in Fig. 1, where (a) represents the experimental data and (b) shows the results of analytical simulation from the model. It is observed that a great amount of energy, defined as the encompassed area in the loops, can be absorbed during each cycle of hysteretic motion of the material and this mechanic behavior is adequately simulated by the analytical model.

Now with the material model ready a 2-D finite element formulation for the viscoelastic damper was derived here. Fig. 2(a) shows an illustration for the proposed damping device to be installed at the joint between the horizontal and the inclined structural members as shown in joint D of Fig. 2(b), and in between the sleeve tubes is the viscoelastic material designed to dissipate the input energy. Because for the viscoelastic layer in between the sleeve tubes, only in-plane motion is allowed while the transverse and the rotational motion are restrained, the viscoelastic dampers are working mostly in a shear motion. Therefore, the element derived here is similar to a joint element. Shown in Fig. 3(a) are the global coordinate system x and y, and local coordinate system ξ and η. The global displacements $\boldsymbol{X}(t)$ are represented by the displacements at nodal point 1 $\boldsymbol{D}_1(t)$ and nodal point 2 $\boldsymbol{D}_2(t)$ as

$$\boldsymbol{X}(t) = \begin{pmatrix} \boldsymbol{D}_1(t) \\ \boldsymbol{D}_2(t) \end{pmatrix} = \begin{pmatrix} a_1(t) \\ a_2(t) \\ a_3(t) \\ a_4(t) \\ a_5(t) \\ a_6(t) \end{pmatrix} \tag{5}$$

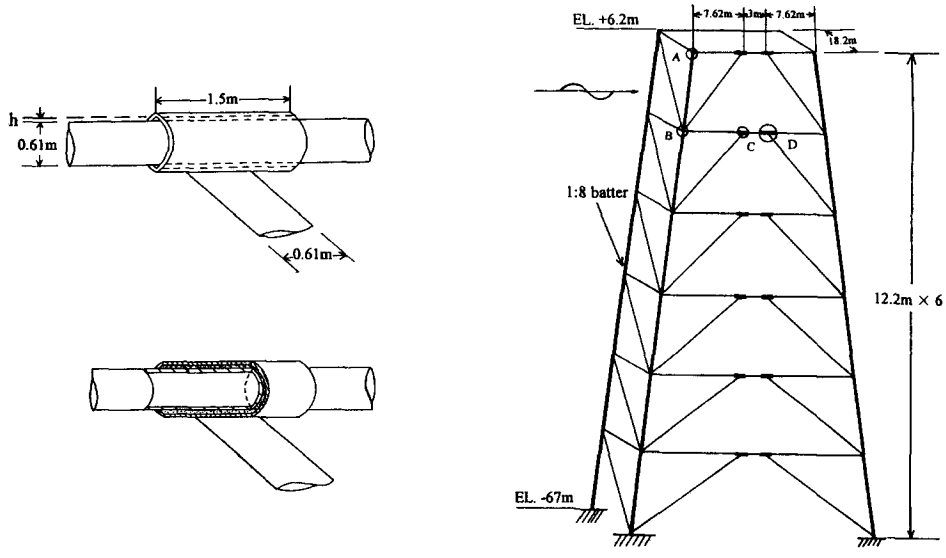

(a) Detailing of the viscoelastic damper (b) Redesigned A-type platform system

Fig. 2 A-type offshore template platform redesigned with damping devices.

where $a_1(t)$ and $a_2(t)$ are global displacements at nodal point 1 in x- and y-directions respectively; $a_4(t)$ and $a_5(t)$ are those at nodal point 2 while $a_3(t)$ and $a_6(t)$ are the rotation at nodal point 1 and nodal point 2 respectively.

As shown in Fig. 3(b) the relative displacement between node 1 and 2 in the transverse direction of the local coordinate system η is defined as

$$\Delta\eta(t)=\eta_2(t)-\eta_1(t)=\boldsymbol{TD}_2(t)-\boldsymbol{TD}_1(t) \tag{6}$$

or in the matrix form

$$\Delta\eta(t)=\boldsymbol{BX}(t) \tag{7}$$

where $\boldsymbol{T}$ is the transformation matrix between the local and global coordinate system, and

$$\boldsymbol{B}=[-\boldsymbol{T}\ \boldsymbol{T}] \tag{8}$$

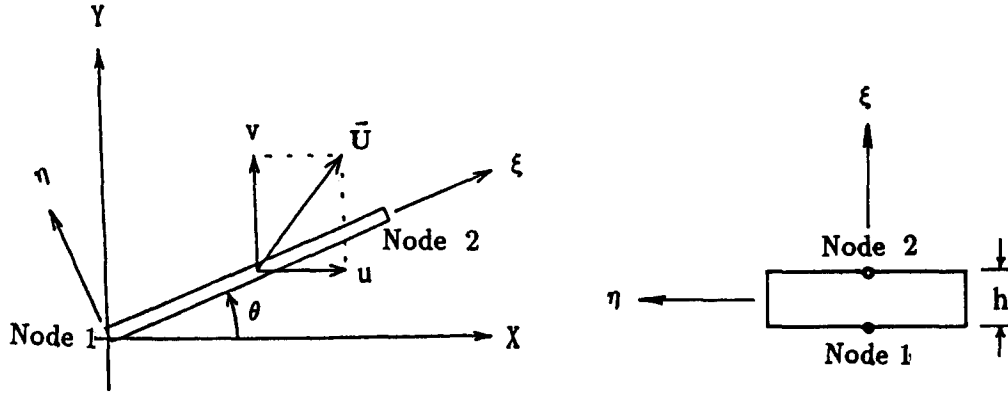

Fig. 3 (a) Local and global coordinate system, (b) Local coordinate system for the damper element.

Then the engineering shear strain of the damping device considered here is given as

$$\gamma(t)=\frac{\Delta\eta(t)}{h} \tag{9}$$

where h is the thickness of the viscoelastic layer. By applying the virtual work principle, the equilibrium resisting force, $F(t)$ resulted from the viscoelastic damper is given by

$$F(t)=B^T\tau(t)A_s \tag{10}$$

where A_s is the shear area of the viscoelastic layer. Combination of Eqs. (1), (2), (7) and Eq. (9) into Eq. (10) leads to a finite element formulation for the viscoelastic damper at time step $t=n\Delta t$ as

$$F(n\Delta t)=K_D X(n\Delta t)+F_p(n\Delta t) \tag{11}$$

where

$$K_D=B^T E_D B \tag{12}$$

is the stiffness matrix, and $F_p(n\Delta t)$ is the previous time effect of the equivalent nodal force presented as

$$F_p(n\Delta t)=B^T\tau_p(n\Delta t)A_s \tag{13}$$

In the stiffness matrix, the modulus E_D becomes

$$E_D=\frac{A_s}{h}\left[G_0+\frac{G_1(\Delta t)^{-\alpha}}{(1-\alpha)\Gamma(1-\alpha)}\right]. \tag{14}$$

3. Offshore structural system under strong ground motion

The dynamic equation of motion for the engineering structural member element with mass M, structural damping C, and stiffness K, subjected to the strong ground motion and the wave forces propagated in the normal direction of the structural member, can be written as

$$M(\ddot{X}(t)+\ddot{X}_g(t))+C\dot{X}(t)+KX(t)=P(t) \tag{15}$$

where $\ddot{X}(t)$, $\dot{X}(t)$ and $X(t)$ are the acceleration, velocity and displacement of the structural member relative to the ground motion respectively, and $\ddot{X}_g(t)$ is the ground acceleration. Taking into account of the relative motion between the structures and fluids, and modified with strong ground motion, the wave forces exerted on the body, $P(t)$ (Newman 1977, Isaacson 1979) are

$$P(t)=\rho C_m V^e\dot{U}_n(t)-\rho C_a V^e(\ddot{X}_n(t)+\ddot{X}_{gn}(t))+\frac{1}{2}\rho C_d A^e\,|U_n(t)-\dot{X}_n(t)|(U_n(t)-\dot{X}_n(t)), \tag{16}$$

where $C_a=C_m-1$, and $U_n(t)$ and $\dot{U}_n(t)$ are the velocity and acceleration of the fluid normal to the structural member resulted from the horizontal and vertical motion of the fluid, respectively. $\ddot{X}_n(t)$ and $\dot{X}_n(t)$ are the acceleration and the velocity of the structural member relative to the ground motion in the normal direction η, and $\ddot{X}_{gn}(t)$ is the ground acceleration in the normal direction η. C_m and C_d are coefficients corresponding to inertia and drag effect respectively. V^e

and A^e are the displaced volume and the projected front area of the structural member, respectively. The last term in the equation representing the drag force due to the relative velocity of fluid is nonlinear. The nonlinearity of the drag term is retained through the use of the approximate relation derived by Penzien and Tseng(1978),

$$|U_n(t)-\dot{X}_n(t)|(U_n(t)-\dot{X}_n(t))=|U_n|U_n(t)-2<|U_n|>\dot{X}_n(t), \tag{17}$$

where $<|U_n|>=\hat{U}_n$ represents the time average of $|U_n|$. Through the substitution of this approximation the wave forces accounted for the ground motion may be represented as

$$P(t)=\rho C_m V^e \dot{U}_n(t)-\rho C_a V^e(\ddot{X}_n(t)+\ddot{X}_{gn}(t))+\frac{1}{2}\rho C_d A^e(|U_n|U_n(t)-2\hat{U}_n\dot{X}_n(t)), \tag{18}$$

Now the normal motion for both structural displacements and fluids at the nodes of the structural member can be transformed through the transformation matrix $\boldsymbol{B}_1$ into the global system, respectively, as

$$\boldsymbol{X}_n(t)=B_1\boldsymbol{X}(t) \tag{19}$$

and

$$\boldsymbol{U}_n(t)=\boldsymbol{B}_1\boldsymbol{U}(t) \tag{20}$$

where $\boldsymbol{X}(t)$ are the nodal displacements and $\boldsymbol{U}(t)$ is the velocity of the fluid particle represented as

$$\boldsymbol{U}(t)=\begin{pmatrix} u_1(t) \\ v_1(t) \\ w_1(t) \\ u_2(t) \\ v_2(t) \\ w_2(t) \end{pmatrix}, \tag{21}$$

with u_1, v_1, u_2, and v_2 representing the horizontal and vertical fluid velocities at node 1 and 2 respectively and w_1 and w_2 being zeros when the irrotational flow is assumed. The transformation matrix $\boldsymbol{B}_1$ is written as

$$\boldsymbol{B}_1=\begin{pmatrix} \boldsymbol{T}_1 & \boldsymbol{0} \\ \boldsymbol{0} & \boldsymbol{T}_1 \end{pmatrix} \tag{22}$$

with

$$\boldsymbol{T}_1=\begin{pmatrix} \sin^2\theta & -\sin\theta\cos\theta & 0 \\ -\sin\theta\cos\theta & \cos^2\theta & 0 \\ 0 & 0 & 1 \end{pmatrix} \tag{23}$$

After the substitution of Eqs. (18) associated with Eqs. (19) and (20), and letting $\boldsymbol{K}^e=\boldsymbol{K}$ Eq. (15) takes the form as

$$\boldsymbol{M}^e\ddot{\boldsymbol{X}}(t)+\boldsymbol{C}^e\dot{\boldsymbol{X}}(t)+\boldsymbol{K}^e\boldsymbol{X}(t)=\boldsymbol{C}_m^e\dot{\boldsymbol{U}}(t)+\boldsymbol{C}_d^e\boldsymbol{U}(t)-\boldsymbol{M}^e\ddot{\boldsymbol{X}}_g(t) \tag{24}$$

where

$$\boldsymbol{M}^e = \boldsymbol{M} + \rho C_a V^e \boldsymbol{B}_1; \tag{25a}$$

$$\boldsymbol{C}^e = \boldsymbol{C} + \rho C_d A^e \hat{\boldsymbol{U}}_n \boldsymbol{B}_1; \tag{25b}$$

$$\boldsymbol{C}_m^e = \rho C_m V^e \boldsymbol{B}_1, \tag{25c}$$

and

$$\boldsymbol{C}_d^e = \frac{1}{2} \rho C_d A^e \mid \boldsymbol{U}_n \mid \boldsymbol{B}_1. \tag{25d}$$

Now if the damping devices are applied, a nonlinear force induced by the viscoelastic dampers might be added to the structural system, and after the combination of equations for each element to the whole system the equations of motion at time step $t=n\Delta t$ take a form as

$$\tilde{\boldsymbol{M}}\ddot{\boldsymbol{X}}(n\Delta t) + \tilde{\boldsymbol{C}}\dot{\boldsymbol{X}}(n\Delta t) + (\tilde{\boldsymbol{K}} + \tilde{\boldsymbol{K}}_D)\boldsymbol{X}(n\Delta t) + \tilde{\boldsymbol{F}}_p(n\Delta t) = \tilde{\boldsymbol{P}}(n\Delta t) \tag{26}$$

where $\tilde{\boldsymbol{M}}$ and $\tilde{\boldsymbol{C}}$ are the global mass and damping matrix respectively while $\tilde{\boldsymbol{K}}$ and $\tilde{\boldsymbol{K}}_D$ are global stiffness matrix corresponding to the stiffness contributed by the regular members and the stiffness resulted from the viscoelastic dampers. $\tilde{\boldsymbol{F}}_p(n\Delta t)$ is the previous time effect from the damping devices installed in the structural system. The global vector of loading resulted from the wave motion and strong ground motion is given as

$$\tilde{\boldsymbol{P}}(n\Delta t) = \tilde{\boldsymbol{C}}_m \dot{\boldsymbol{U}}(n\Delta t) + \tilde{\boldsymbol{C}}_d \boldsymbol{U}(n\Delta t) - \tilde{\boldsymbol{M}}\ddot{\boldsymbol{X}}_g(n\Delta t) \tag{27}$$

For the offshore template structure located in the ocean with a ratio of depth and wave length over 1/10, the Stokes wave theory of fifth-order (Skjelbreia and Hendrickson 1960) is usually applied. Therefore, in this study the velocity and acceleration of the fluids are based on the Stokes fifth-order wave theory. The horizontal and vertical velocity, u and v for a point located at (x, y) are presented, respectively, as

$$u = \frac{\omega}{k} \sum_{m=1}^{5} G_m \frac{\cosh mky}{\sinh mkd} \cos m(kx - \omega t) = \frac{\omega}{k} \sum_{m=1}^{5} U_m \cos m(kx - \omega t), \tag{28a}$$

and

$$v = \frac{\omega}{k} \sum_{m=1}^{5} G_m \frac{\sinh mky}{\sinh mkd} \sin m(kx - \omega t) = \frac{\omega}{k} \sum_{m=1}^{5} V_m \sin m(kx - \omega t), \tag{28b}$$

where k=wave numbers; ω=angular frequency; d=water depth, and U_m and V_m are obtained from G_m the parameters corresponding to water depth, wave numbers and wave length (Skjelbreia and Hendrickson 1960). The horizontal and vertical acceleration of the fluids are accordingly obtained through the first time derivative of the velocities as $\dot{u}$ and $\dot{v}$.

Now having the equations of motion and the forces exerted on the structural system ready, the analysis can be carried out by using the step-by-step integration schemes for the nonlinear structural system such as Newmark-β method (Newmark 1962) and Wilson's method (Bathe and Wilson 1976). In this study the Newmark method using average acceleration operator was adopted due to its stability advantage.

4. Numerical results and discussion

In the numerical analysis, a typical 6-story, 1-bay A-type template platform as shown in Fig.

2, was selected and redesigned with damping devices at the joint between the horizontal and inclined bracing members, where the detail of the damping devices were shown in Fig. 2(a). The diameters and the thickness of the structural members are 1.22 m and 38.0 mm for the vertical members and 0.61 m and 19.0 mm for the horizontal and bracing members respectively. During this stage of analysis the foundation of the platform was assumed to be clamped on the sea floor and the density of the structural material and water were 7.8×10^3 kg/m^3 and 1.02×10^3 kg/m^3 respectively. The mass applied on the deck was assumed to be 428.0 ton and uniformly distributed.

The viscoelastic dampers used in the analysis have typical coefficients as follows: G_0=G_1= 662.0 kPa, α=0.75. The geometrical dimensions for the dampers are: h=2.54 cm and b=1.50 m. To simplify the analysis, the degradation of the damper stiffness resulted from the energy absorption was not taken into consideration during this stage of analysis. To be able to reflect the damping effect that is solely resulted from the added damping devices the system damping was ignored in the analysis. Three types of loading were applied to the offshore structure, namely the step loading, wave forces and strong ground motions similar to earthquakes. The analysis was focused on the displacement induced by the input loading and the effect of displacement reduction when the viscoelastic dampers were applied. The results were obtained by carrying out the calculation for the coupled MDOF nonlinear system, and then were plotted and represented in figures, where the dotted curves represent the undamped responses while the solid curves represent damped responses.

4.1. Step loading analysis

In the step loading analysis a 0.1 g ground motion was assumed to be suddenly exerted on the foundation of the structure and then sustained for the rest of time. Figs. 4(a) and (b) showed the response comparisons of the horizontal displacement and rotation respectively, between the traditional designed and new designed offshore structure, at the corner joint of the top deck as marked in the sketch of the structure as joint A. Figs. 5(a) and (b) showed the response comparisons for the horizontal and vertical displacement at joint B, the level next to the top deck. The responses in the top deck are generally larger than those in the lower levels as was shown in Figs. 4(a) and Fig. 5(a), where the horizontal displacement response for the top deck is about

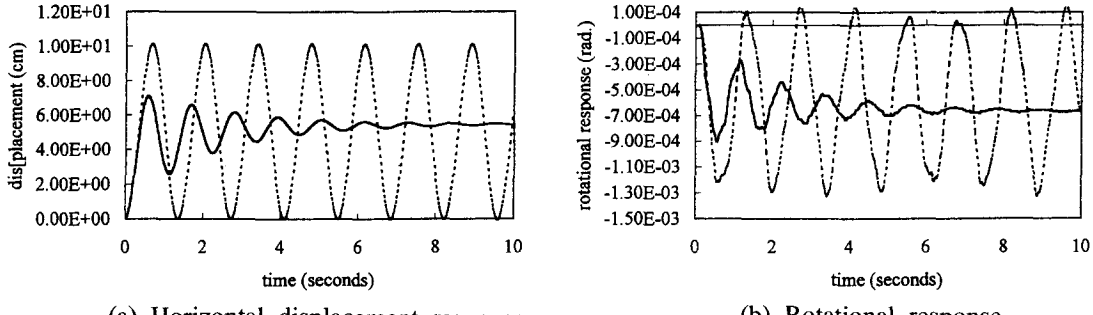

(a) Horizontal displacement response

(b) Rotational response

Fig. 4 Response comparison for joint A under step loading.

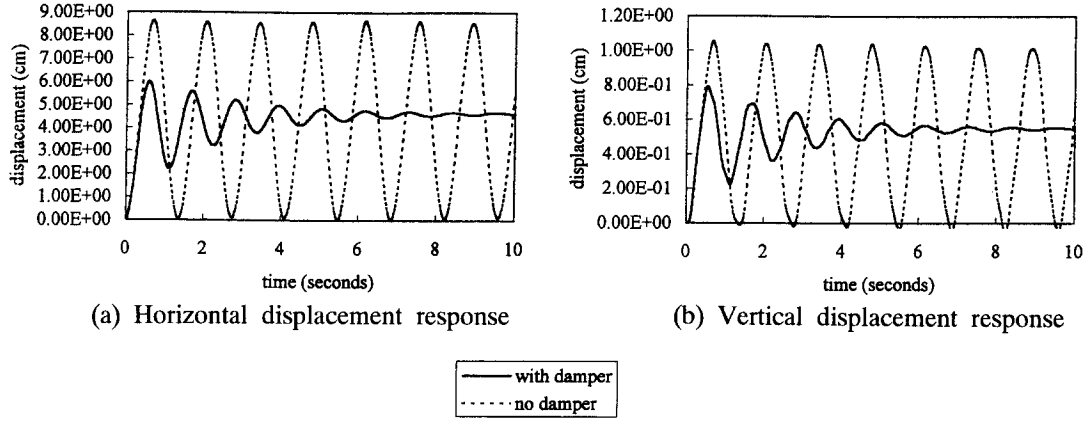

(a) Horizontal displacement response (b) Vertical displacement response

Fig. 5 Response comparison for joint B under step loading.

10% higher than that of the level next to the top. For each response comparison an early reduction for the responses of the redesigned offshore structural system was observed, and then the responses were flattened gradually to an amplitude corresponding to the static responses. It is also found that the system stiffness for the new designed structural system is compatible to the traditional designed structure, and the dominant frequency for this A-type offshore structural system is about 0.73 Hz.

4.2. Wave force analysis

In the wave force analysis the wave forces adopted were based on the Stokes fifth order theory for a wave of 90 m long and 6.0 m high traveling in a water of 67 m deep. Figs. 6(a), (b) and (c) showed the comparisons of the wave induced response corresponding to the horizontal, vertical displacement and the rotational response for joint A as marked in the sketch of the structure while Figs. 7(a), (b) and (c) showed the response comparisons of structure at joint B corresponding to the horizontal, vertical and rotational motion. A significant reduction on the vibration amplitude due to the viscoelastic damping was again realized as shown in these figures when the platform was subjected to the wave motions. Curves corresponding to the displacement and the rotation in the structure incorporated with damping devices are more smooth and flat.

An additional analysis was performed for the platform with reduced dimensions of structural members, in which the thickness of all structural members and the length of the joint sleeves with damping material were reduced into half. Figs. 8(a), (b) and (c) showed the response comparisons of structure at joint A corresponding to the horizontal, vertical and rotational motion. The behavior of the structure with thinner tube members subjected to the wave motions was generally similar to the structure with full scale of structural members, except that a larger amplitude associated with lower frequency was observed.

4.3. Earthquake loading analysis

For the earthquake loading analysis two strong ground motions similar to the actual earthquakes were applied to the A-type offshore structure. The first acceleration time history is similar to the 1940 El Centro earthquake and the second is similar to the 1985 Mexico earthquake.

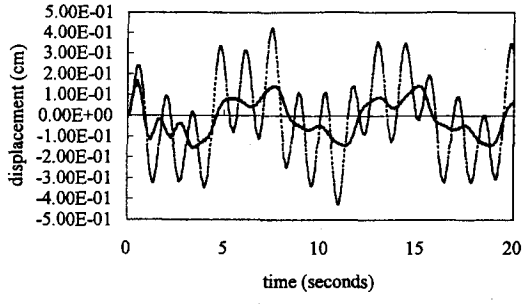

(a) Horizontal displacement response

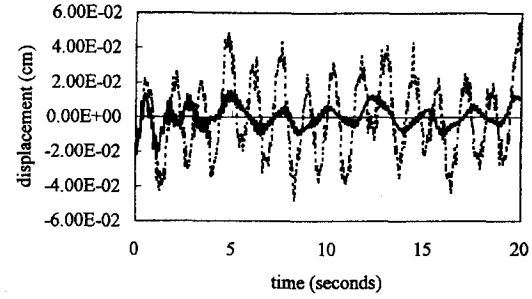

(b) Vertical displacement response

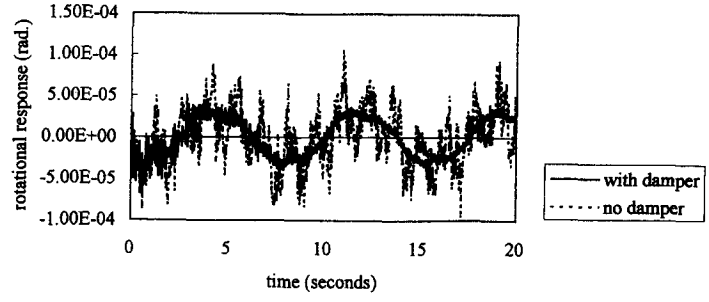

(c) Rotational response

Fig. 6 Response comparison for joint A subjected to wave forces.

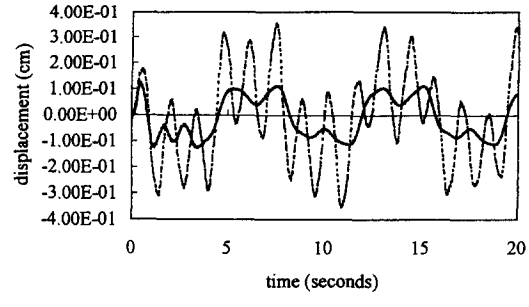

(a) Horizontal displacement response

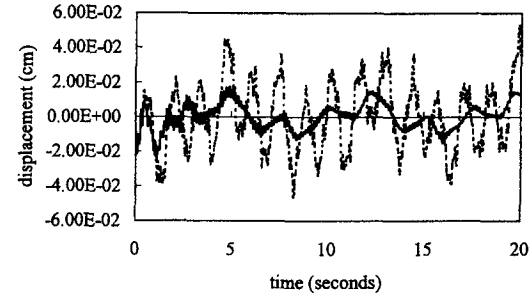

(b) Vertical displacement response

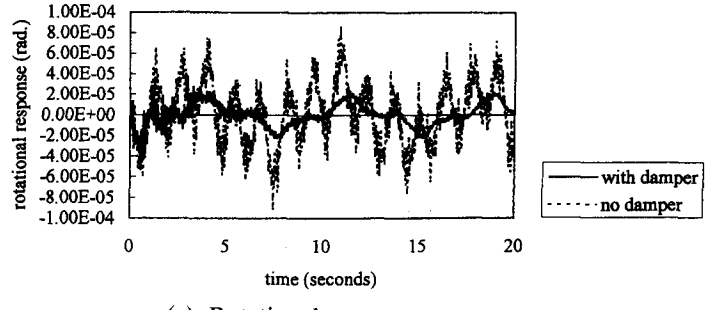

(c) Rotational response

Fig. 7 Response comparison for joint B subjected to wave forces.

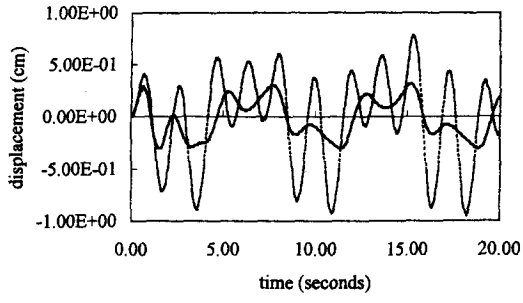

(a) Horizontal displacement response

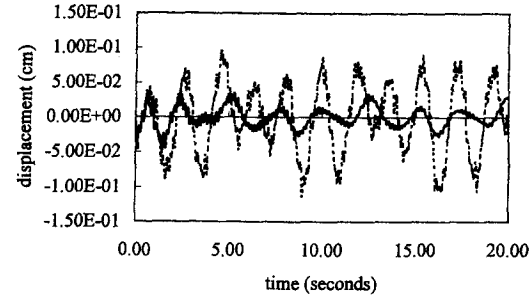

(b) Vertical displacement response

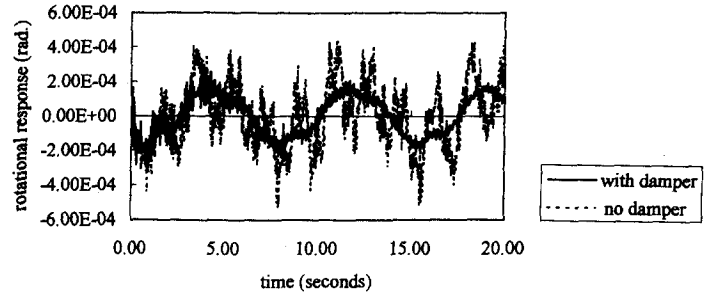

(c) Rotational response

Fig. 8 Response comparison for joint A of structure with thinner members subjected to wave forces.

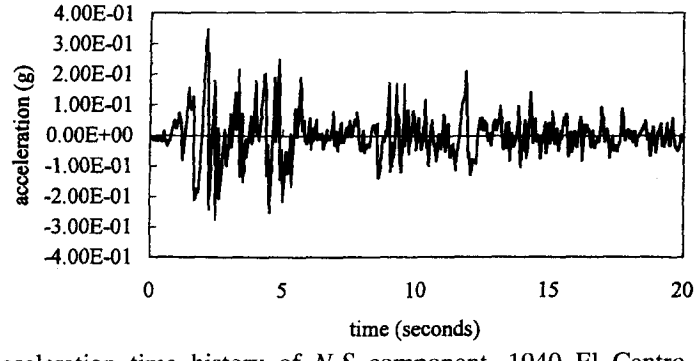

Fig. 9 Acceleration time history of *N-S* component, 1940 El Centro earthquake.

Fig. 9 showed the first 20 seconds time history of the ground motion for the *N-S* component of 1940 El Centro earthquake, where the maximum amplitude is 0.34 g. Fig. 10(a), (b) and (c) showed the response comparisons of the horizontal, vertical displacement and the rotation at joint A when the structure subjected to the first strong ground motions. Illustrated in Fig. 11(a), (b) and (c) are the response comparisons for the joint B when the same ground motions were applied. It was observed in these figures that during the early loading stages, earlier than about the 7-th second, the responses between the traditional designed and the new designed structure were compatible to each other while after then the mitigation effect resulted from the damping devices was getting more and more significant. The stress-strain curves during the response history for

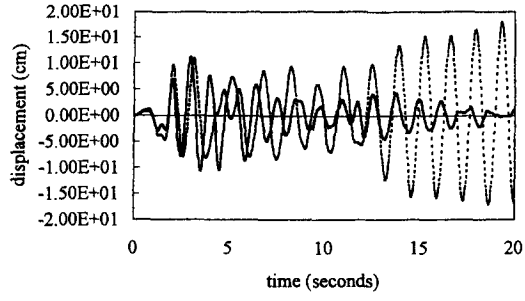

(a) Horizontal displacement response

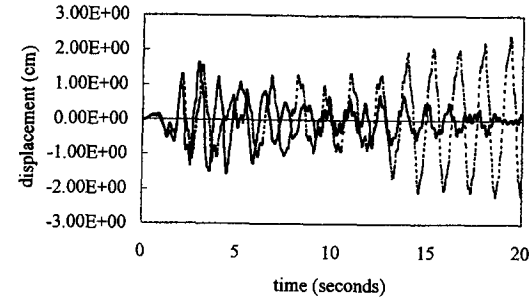

(b) Vertical displacement response

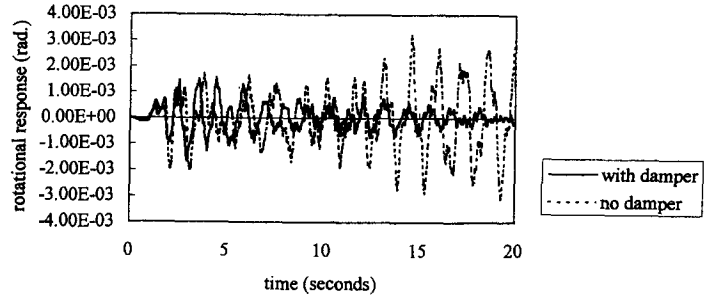

(c) Rotational response

Fig. 10 Response comparison for joint A subjected to strong ground motion 1.

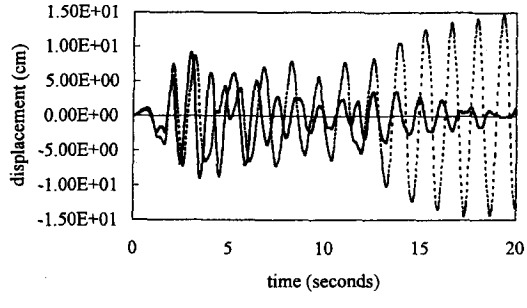

(a) Horizontal displacement response

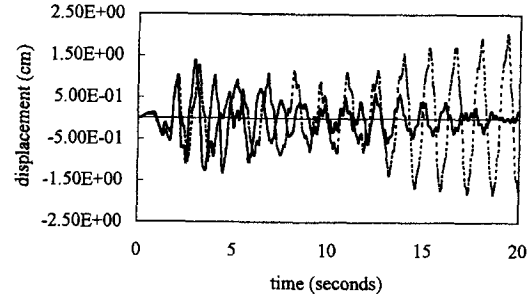

(b) Vertical displacement response

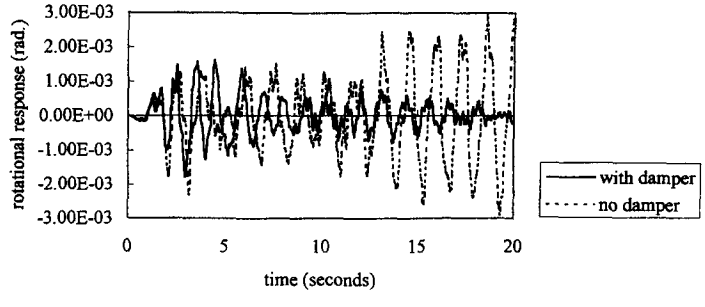

(c) Rotational response

Fig. 11 Response comparison for joint B subjected to strong ground motion 1

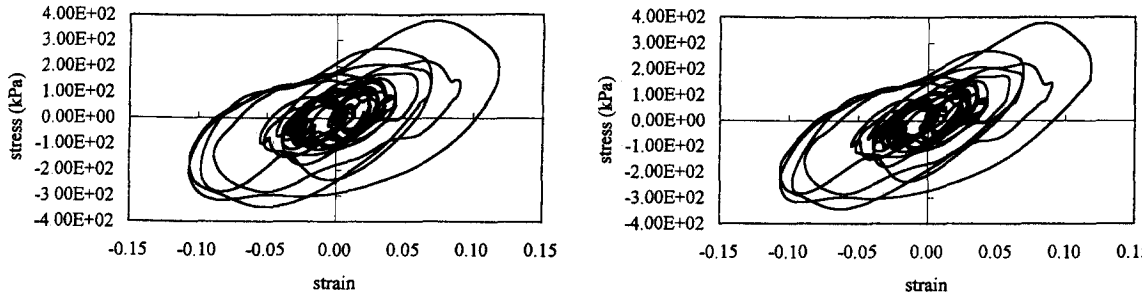

(a) Response for damper at joint C

(b) Response for damper at joint D

Fig. 12 Stress-strain curves for the viscoelastic damping material under strong ground motion 1.

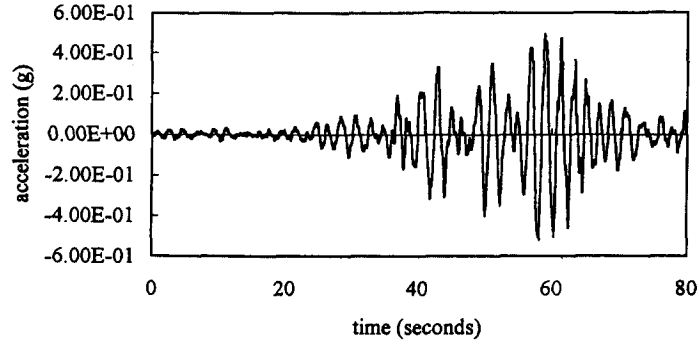

Fig. 13 Acceleration time history of *N-W* component, 1985 Mexico earthquake.

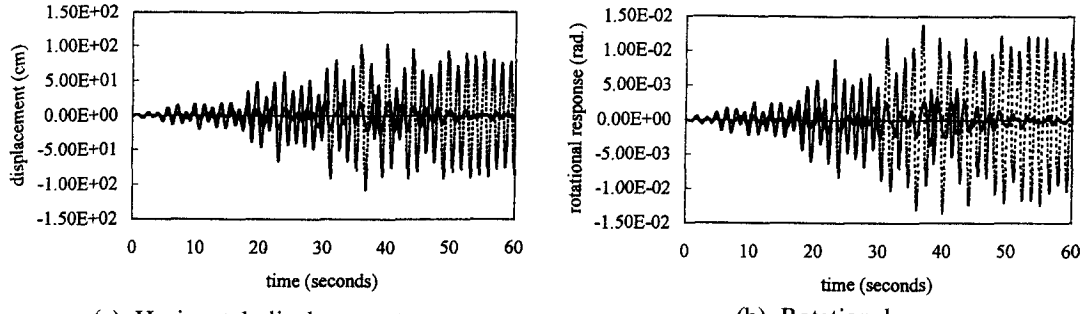

(a) Horizontal displacement response

(b) Rotational response

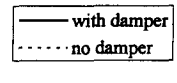

Fig. 14 Response comparison for joint A subjected to strong ground motion 2

the damper at joint C and joint D were also presented in Figs. 12(a) and (b) respectively. It showed a typical viscoelastic material behavior as illustrated in Fig. 1, the experimental testing results.

Fig. 13 showed the second accelerogram of strong ground motion similar to the *N-W* component of 1985 Mexico earthquake, where the time history from the 20-th second to 80-th

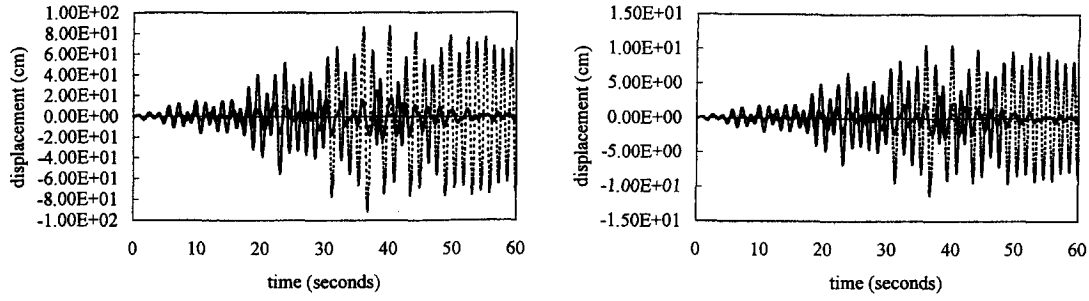

(a) Horizontal displacement response (b) Vertical displacement response

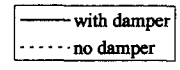

Fig. 15 Response comparison for joint B subjected to strong ground motion 2

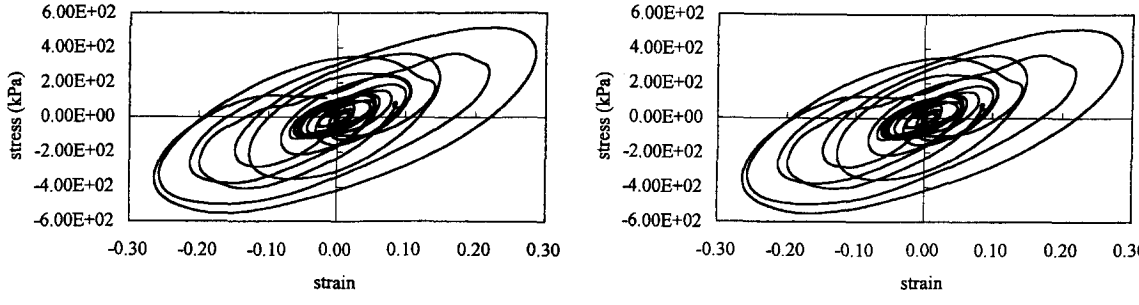

(a) Response for damper at joint C (b) Response for damper at joint D

Fig. 16 Stress-strain curves for the viscoelastic damping material under strong ground motion 2

second was adopted for the analysis and the maximum magnitude was 0.52 g. Figs. 14(a) and (b) showed the response comparisons of the horizontal displacement and rotation at joint A when the second strong ground motion was exerted on the structure while Figs. 15(a) and (b) showed the comparisons for the horizontal and vertical displacement for joint B. Again as was shown in the first example for the earthquake motion, the amplitudes of each response time history were reduced significantly, even more significant when compared to the first earthquake application. Figs. 16(a) and (b) showed the stress-strain relationships for the viscoelastic damping devices installed at joint C and joint D respectively during the second earthquake response time history for the first 30 seconds of the analysis. Again a typical viscoelastic material behavior was realized in the hysteretic loops while the encompassed area in the loops was relatively larger than in the loops obtained in the first case of earthquake loading.

5. Conclusions

As was shown in the analysis, it is concluded that the viscoelastic damper can be effectively applied to the A-type offshore structure and the vibration of the structure induced by both the wave forces and the strong ground motions can be reduced to a satisfactory degree. In most

cases the vibration amplitude of the structure can be reduced by more than 50%, and in the extreme cases such as in the earthquake loading analysis the reduction of the vibration resulted from the viscoelastic damping devices can even reach a higher percentage. The analytical results showed that not only did the amplitude of the responses be reduced dramatically but also the high frequency vibration mode was filtered into a lower frequency mode such as the high mode vertical and rotational vibration. The advantage of this improved design approach to install the viscoelastic damping devices as a sleeve joint in between the horizontal and inclined members is also obvious. This method may well avoid the stability problem that might occur in the diagonal bracing, which is separated into two parts by the viscoelastic damping devices installed in the old method. It is encouraged that the application of the viscoelastic dampers to the A-type offshore structural system may effectively upgrade the dynamic characteristics for the structure under both the rough marine environment and the strong ground motion from earthquakes.

References

Bagley, R.H. and Torvik, P.J. (1979), "A generalized derivative model for an elastomer damper", *Shock Vibration Bull.*, **49**, 135-143.

Bathe, K.J. and Wilson, E.L. (1976), *Numerical Methods in Finite Element Analysis*, Prentice-Hall, Englewood Cliffs, NJ.

Bergman, D.M. and Hanson, R.D. (1986), "Characteristics of viscoelastic damping devices", *Proc. ATC Seminar and Workshop on Base Isolation and Passive Energy Dissipation*, Applied Technology Council, Redwood City, CA.

Isaacson, M. (1979), "Nonlinear inertia forces on bodies", *J. Waterways etc., Div. ASCE*, WW3, 213-227.

Chang, K.C., Soong, T.T., Oh, S.T. and Lai, M.L. (1991), "Seismic response of a 2/5 scale steel structure with added viscoelastic dampers", *Technical Report NCEER-91-0012*, State University at Buffalo, Buffalo, NY.

Lee, H.H. and Tsai, C.S. (1992), "Analytical model for viscoelastic dampers in seismic mitigation application", *10th World Conf. on Earthquake Engrg.*, Madrid Spain., 2461-2466.

Lee, H.H. and Tsai, C.S. (1994), "Analytical model of viscoelastic dampers for seismic mitigation of structures", *Computers and Structures-An Int. J.*, **50**(1), 111-121.

Lee, H.H. and Wu, R.-J. (1996), "Vibration mitigation of structures in the marine environment", *Ocean Engineering-An Int. J.*, **23**.

Lin, R.C., Liang, Z. and Soong, T.T. (1988), "An experimental study of seismic structural response with added viscoelastic dampers", *Technical Report NCEER-88-0018*, State University at Buffalo, Buffalo, NY.

Mahmoodi, P. (1972), "Structural dampers", *J. Structural Div., ASCE* **95**, 1661-1667.

Mason, A.B., Beck, J.L., Chen, J. and Ullmann, R.R. (1989), "Modal parameter identification of an offshore platform from earthquake response records", *Seismic Engineering: Research and Practice-Proceedings, Seismic Engineering at Structure Congress*, Edited by Kircher, A. and Choppra, A.K. 217-226.

Newman, J.N. (1977), *Marine Hydrodynamics*, MIT Press, Camn. Mass.

Newmark, N.M. (1962). "A method of computation for structural dynamics", *Trans. ASCE,* **127**(1), 1406-1435.

Penzien, J. and Tseng, S. (1978), "Three-dimensional dynamic analysis of fixed offshore platforms", In *Numerical Methods in Offshore Engineering*, John Wiley and Sons, New York, 221-243.

Skjelbreia, L. and Hendrickson, J.A. (1960), "Fifth order gravity wave theory", *Proc. 7th Coastal Eng. Conf.*, The Hague, 184-196.

Tsai, C.-S. and Lee, H.H. (1992a), "Application of viscoelastic dampers to jointed structures for seismic mitigation", *ASCE Engineering Mechanics Conference*, Texas A & M University.

Tsai, C.-S. and Lee, H.H. (1992b), "Application of viscoelastic dampers to bridges for seismic mitigation",

PVP Vol. 229, Doe Facilities Programs, System Interaction and Active/Interactive Damping ASME, 113-118.

Tsai, C.-S. and Lee, H.H. (1993a), "Application of viscoelastic dampers to high-rise buildings", *J. of Structural Engineering, ASCE,* **119**(4), 1222-1233.

Tsai, C.-S. and Lee, H.H. (1993b), "Seismic mitigation of bridges by using viscoelastic dampers", *Computers and Structures-An Int. J.,* **48**(4), 719-727.

PVP **229**, *Doe Facilities Programs, System Interaction and Active/Interactive Damping ASME*, 113-118.

Tsai, C.-S. and Lee, H.H. (1993a), "Application of viscoelastic dampers to high-rise buildings", *J. of Structural Engineering ASCE*, **119**(4), 1222-1233.

Tsai, C.-S. and Lee, H.H. (1993b), "Seismic mitigation of bridges by using viscoelastic dampers", *Computers and Structures, An Int'l J.* **48**(4), 719-727.